Published in final edited form as:
Magn Reson Med. 2011 December ; 66(6): 1674–1681. doi:10.1002/mrm.22950.

*Co*mpressed-Sensing *Mo*tion Compensation (CosMo): A Joint Prospective-Retrospective Respiratory Navigator for Coronary MRI

Mehdi H. Moghari[1], **Mehmet Akçakaya**[1], **Alan O'Connor**[1,3], **Tamer A. Basha**[1], **Michele Casanova**[1], **Douglas Stanton**[4], **Lois Goepfert**[1], **Kraig V. Kissinger**[1], **Beth Goddu**[1], **Michael L. Chuang**[1], **Vahid Tarokh**[3], **Warren J. Manning**[1,2], and **Reza Nezafat**[1]

[1] Department of Medicine (Cardiovascular Division), Harvard Medical School and Beth Israel Deaconess Medical Center, Boston, MA

[2] Department of Radiology, Harvard Medical School and Beth Israel Deaconess Medical Center, Boston, MA

[3] School of Engineering and Applied Sciences, Harvard University

[4] Philips Research North America, Briarcliff Manor, NY

Abstract

Prospective right hemi-diaphragm navigator is commonly used in free-breathing coronary MRI. The navigator results in an increase in acquisition time to allow for re-sampling of the motion-corrupted k-space data. In this study, we are presenting a joint prospective-retrospective navigator motion compensation algorithm called *co*mpressed-sensing *mo*tion compensation (CosMo). The inner k-space region is acquired using a prospective navigator; for the outer k-space, a navigator is only used to reject the motion-corrupted data without reacquiring them. Subsequently, those unfilled k-space lines are retrospectively estimated using compressed sensing (CS) reconstruction. We imaged right coronary artery (RCA) in 9 healthy adult subjects. An under-sampling probability map and sidelobe-to-peak ratio (SPR) were calculated to study the pattern of under-sampling, generated by navigator. RCA images were then retrospectively reconstructed using CosMo for gating windows between 3–10 mm and compared with the ones fully acquired within the gating windows. Qualitative imaging score and quantitative vessel sharpness were calculated for each reconstruction. The probability map and SPR show the navigator generates a random under-sampling k-space pattern. There were no statistically significant differences between the vessel sharpness and subjective score of the two reconstructions. CosMo could be an alternative motion compensation technique for free-breathing coronary MRI that can be used to reduce scan time.

Keywords

coronary MRI; motion correction; diaphragmatic navigators; compressed sensing

INTRODUCTION

Respiratory and cardiac motions are the main challenges of high resolution coronary MRI (1). For cardiac motion, a patient specific rest period during the cardiac cycle is commonly

Correspondence to: Reza Nezafat, Ph.D., Beth Israel Deaconess Medical Center, 330 Brookline Ave, Boston, MA, 02215, Phone: 617-667-1747; Fax: 617-975-5480, rnezafat@bidmc.harvard.edu.

employed (2). While breath-hold acquisitions have been previously used in coronary MRI (3–4), the limited breath-hold duration constraints spatial resolution and the clinical applicability of this approach. Despite several advances over the past two decades, respiratory motion still remains a major challenge.

Various methods exist for respiratory motion monitoring and compensation. Respiratory navigators (NAV) were developed a decade ago and have been continuously refined to become the most reliable respiratory motion compensation technique for free-breathing coronary MRI (5–7). A two dimensional (2D) pencil-beam or spin echo with orthogonal planes for excitation and refocusing, positioned on the right hemi-diaphragm, is used to monitor the respiratory motion. In prospective acceptance-rejection NAV gating (8–9), the k-space segment, acquired immediately following the NAV, is accepted if the NAV is within a pre-specified acceptance gating window. Otherwise, data are discarded, and reacquired in the next cardiac cycle. This results in an acceptance efficiency of 30–80%. A larger gating window improves data acquisition efficiency, albeit with the penalty of accepting more motion-corrupted k-space. Multiple methods have been proposed to improve NAV motion detection capability and acquisition efficiency which are comprehensively reviewed by Scott et. al. (1). Examples of such advancements include fat NAV as a surrogate for direct coronary motion (10–11), leading and trailing NAV (7), and continuously adaptive windowing strategy to improve acquisition efficiency (12). Image or projection-based methods have also been presented to compensate for respiratory motion (13–15). In projection-based techniques, the motion of the heart directly measured from acquired raw data is used to calculate the respiratory motion. In image-based techniques, a low resolution image is commonly extracted from the central portion of k-space and used for retrospectively compensating the respiratory motion (16–18). Rigid body and affine transformations can also be employed for prospectively correcting the respiratory motion and increasing the gating window and efficiency rate (19–21). While prospective acquisition is commonly used for coronary MRI, there have been also some studies of using a retrospective NAV gating with the aim of improving gating efficiency or completion of scan in a fixed amount of time (22–23).

Utility of compressed sensing for estimating motion-corrupted data was presented for removing swallowing artifacts in larynx imaging (24). A pseudo-random trajectory was designed to generate a motion-free under-sampled k-space from the information provided by NAV. The under-sampled k-space of larynx was then used in the standard CS algorithm (25) to estimate the unfilled k-space data. In cardiac MR, the quasi-periodic nature of the respiratory pattern yields a randomly undersampled k-space. Therefore, CS reconstruction could potentially be used to estimate the motion-corrupted k-space data without reacquiring them. In this study, we have proposed and evaluated a joint retrospective-prospective NAV gating approach, *Co*mpressed *S*ensing *Mo*tion compensation (CosMo) for coronary MRI. Imaging using a non-rigid motion phantom and in vivo coronary MRI were used to evaluate the efficacy of the proposed respiratory motion technique.

MATERIALS AND METHODS

Figure 1 shows the proposed CosMo data acquisition strategy. The k-space segments are divided into inner and outer regions, which are acquired using two different approaches. The inner k-space segments are first fully acquired using a diaphragmatic NAV with a predefined gating window, similar to the prospective NAV acquisition. The outer k-space segments are accepted for image reconstruction only if the NAV position is within the gating window at the time of their acquisitions; otherwise the k-space segments are discarded and *not* reacquired. Upon completion of the scan, the inner segments are fully sampled, while the outer k-space is under-sampled. The pattern of under-sampling is

enforced by NAV and respiratory motion of a subject. We hypothesize that this under-sampling pattern is random, and methods such as compressed sensing (CS) (25–26) can be used to estimate the motion-corrupted k-space segments.

This study is divided into two sections: 1) to investigate the randomness and incoherence of the NAV-generated under-sampling pattern, and 2) to investigate the efficacy of CosMo for respiratory motion compensation in coronary MRI. Initially, the feasibility of CosMo is studied on a respiratory motion phantom. Then, in a retrospective study, the randomness and incoherence of the generated k-space under-sampling pattern in 3D coronary MRI with the proposed acquisition strategy is investigated. Finally, the generated under-sampling k-space data are reconstructed for different gating windows and compared with the images from fully-sampled data.

Non-rigid Respiratory Phantom Study

To investigate the feasibility of the proposed method, we first performed a phantom study on our pneumatic MR-compatible respiratory and cardiac motion phantom of a two-chamber deformable human heart. The phantom allows for respiratory motion along superior-inferior (SI), and anterior-posterior (AP) directions, however, only SI respiratory motion was used in our experiments. The desired respiratory motion of the phantom, generated from a subject's respiratory motion, was programmed into a microprocessor. The microprocessor controls the motion of the phantom outside the magnet room using a fiber optic cable. The phantom was imaged with an ECG triggered, 3D axial, SSFP sequence with the following parameters: TR/TE = 5.0/2.0 ms; field of view (FoV) = 300×300×112 mm^3; spatial resolution 1.3×1.3×1.5 mm^3; flip angle = 90o. A 2D pencil-beam NAV was placed at the edge of the plate moving the heart, to measure the displacement along SI direction. The acquisition was obtained using 22 phase-encode lines per segment. At the beginning of the scan, the first 20 cardiac cycles were used as a training phase to define the center of 5 mm gating window. The inner k-space lines ($k_y \times k_z$ of 37×26) were fully acquired within this gating window while the outer k-space lines were acquired with 100 mm gating window. A centric profile ordering was used for acquiring the inner k-space segments. After acquiring the inner k-space segments, the profile ordering was changed to the standard radial spokes for acquisition of the rest of k-space segments. For outer k-space, only data within the acceptance window were used for image reconstruction. A fully-sampled reference image with prospective NAV acquisition was also acquired.

Image Reconstruction

After generating the fully sampled and randomly under-sampled 3D k-space datasets, the under-sampled dataset was reconstructed using the modified CS approach (27) called Low-dimensional-Structure Self-Learning and Thresholding (LOST). Minimization of the convex l_1 norm of transform domain coefficients has been the preferred CS sparsity regularization in MRI. This technique assumes that an image has a sufficiently sparse representation in a pre-selected transform domain. Although sparsity is a necessary condition for l_1 norm reconstruction, it is not possible to know whether a transform can efficiently represent the underlying image characteristics. Furthermore, the relevant anatomical features are not necessarily captured in a sparse manner with a fixed transform. LOST, on the other hand, utilizes the structure and anatomical features in the image being reconstructed. By using the information from the image itself, it is able to represent various anatomical features of the image sparsely in an adaptive fashion, without the need for training data. This adaptive representation allows for the removal of aliasing artifacts and noise using thresholding approaches, without causing significant reconstruction artifacts and blurring (27). Therefore, in this study, we have used LOST to estimate the motion-corrupted k-space segment in CosMo.

The proposed method was implemented in MATLAB (The MathWorks, Natick, MA) and C ++ using the FFTW library, for off-line reconstruction. The final estimate is generated by root-sum-squares of the coil estimates.

Coronary MRI Acquisition

Nine healthy adult subjects (3 males, 25 ± 12 years), without any contraindications to MRI, were recruited for this study. All images were acquired using a 1.5T scanner (Achieva, Philips Healthcare, Best, the Netherlands) and a 5-channel phased array coil. Written informed consent was obtained from all the participants and the imaging protocol was approved by our Institutional Review Board.

In each scan, scout images were acquired to localize the anatomy using a balanced steady-state free precession (SSFP) sequence with 3.1 × 3.1 mm^2 in-plane resolution and 10 mm slice thickness. On the scout image, a 2D pencil-beam NAV was placed at the dome of the right hemi-diaphragm. To measure the coil sensitivity maps, a set of reference images were acquired using both the body and the phased array coils. The coil sensitivity maps were used for subsequent acquisitions, but not in LOST reconstruction. The scan was followed by an axial breath-hold cine SSFP sequence with 1.2 × 1.2 mm^2 in-plane resolution and 48 ms temporal resolution, to visually identify the rest period of the right coronary artery (RCA). A low resolution 3D coronary survey volume was next acquired to define an oblique imaging slab covering the RCA. The oblique imaging plane was employed to acquire a free-breathing 3D ECG-gated SSFP sequence with the following parameters: 270×270×30 mm^3 FoV; 1.0×1.0×3.0 mm^3 spatial resolution; TE/TR = 2.6/5.3 ms; flip angle 90o; number of k-space segments measured per shot = 17; NAV gating window 100 mm, i.e. efficiency of 100%; number of averages = 10. Both NAV signal and raw k-space data were recorded and transferred to a stand-alone workstation for further retrospective analysis and reconstruction.

NAV-generated Under-sampling

To study the under-sampling pattern generated by NAV, we retrospectively analyzed the acquired data. For each subject, we had 10 averages and corresponding NAV positions for each segment. To verify the randomness of the accepted k-space segments for each average, a probability map was generated. The probability map shows the acceptance probability of a specific k-space segment within a predefined gating window over ten averages. This probability changes from zero, the case where the k-space segment is not acquired over 10 averages, to 1, for the case where the segment is acquired in all the averages. Had the generated under-sampling pattern been the same at each average, i.e., a deterministic under-sampling pattern, the generated probability map would have only values of either zero or one. Otherwise, if the under-sampling pattern was random, the probability map would have values ranging from 0 to 1. In the generated probability map, the k-space segments having the probability of 0.5 had the maximum randomness over 10 averages.

We used the sidelobe-to-peak ratio (SPR) (25) to investigate the incoherence of the resulting under-sampling pattern. We calculated the point spread functions (PSF) of the under-sampled k-spaces generated for 5 mm gating window for each subject. The SPR was then calculated as the ratio of the second highest peak to the maximum peak of the PSF. A lower SPR suggests an incoherent random sampling pattern. In our analysis, due to the breathing pattern, the gating efficiency for different averages was different. This fact, along with the pattern of the undersampled k-spaces, results in different values for SPR (10 per subject for a total of 90 SPR for all subjects).

The probability map and computed SPR respectively evaluate the randomness and incoherence of the under-sampling k-space patterns that are generated by the respiratory motion measured by NAV.

Retrospective Coronary MRI

A retrospective NAV gated image dataset was reconstructed as a *reference* from the acquired datasets. To fill in the k-space, k-space lines from the first average were included if the associated NAV signal, acquired prior the k-space lines, was within the predefined acceptance window determined during a training phase. For the unfilled k-space lines in the k-space, the data from the subsequent averages was used. The k-space only contains one instance of the accepted k-space segments from all the 9 averages and the remainder of the data was discarded. Four different references were reconstructed for gating windows of 3, 5, 7, and 10 mm. Additionally, another retrospectively gated reference was generated by using a variable gating window of 5 and 10 mm for the inner (the inner 50% of k-space) and the outer (the outer 50% of k-space) k-space segments, respectively.

To create the CosMo k-space data, the k-space was divided into two regions: inner and outer. For inner region, the k-space data were selected similar to the retrospective NAV gated dataset. For outer region the k-space data acquired in the first average was included in the final k-space data if it is within the acceptance window, otherwise these segments were unfilled. This procedure results in the k-space data, which is fully sampled in the inner region while containing randomly distributed unfilled data in the outer region. Similar to the retrospective data, only one instance of each k-space segment was included.

Image Analysis

For each of the 9 subjects, we retrospectively reconstructed coronary images by gating the respiratory motion and using CosMo for different gating windows. Qualitative assessment of coronary artery images was performed by an experienced independent blinded reader using a four-point scale system as previously described in (28): 1, indicating poor or un-interpretable (coronary artery visible, with markedly blurred borders or edges); 2, fair (coronary artery visible, with moderately blurred borders or edges); 3, acceptable (coronary artery visible, with mildly blurred borders or edges); or 4, excellent (coronary artery visible, with sharply defined borders or edges). For each image, separate scores were given for the proximal, mid, and distal segments. The Soap Bubble (29) (Philips Healthcare, Best, the Netherlands) tool was used to quantitatively evaluate the vessel definition. Vessel sharpness scores were calculated for both sides of the vessel and final sharpness was defined as the average score of the both sides. The final normalized sharpness was defined as the average score of the both sides divided by the lumen signal.

Statistical Analysis

All measurements are presented as mean ± one standard deviation. A two tailed, paired Student t-test was used for comparing image quality in all the measurements except the visual grading. A paired two-sided Wilcoxon test was performed for the visual grading. A p-value of <0.05 was considered statistically significant.

RESULTS

Non-rigid Respiratory Phantom Study

Figure 2 depicts the reconstructed images of the respiratory motion phantom using CosMo compared with the prospective NAV gating; zero-filled and motion-corrupted images. CosMo improves visualization of the motion phantom and preserve the sharp edges between the heart and distillated water despite using only 51% of the k-space data.

Coronary MRI

Figure 3 shows the NAV-generated probability map of the accepted k_y-k_z lines over 10 averages of 4 healthy subjects (A-D) for gating windows of 3, 5, 7, and 10 mm, respectively. The under-sampled locations exhibit randomness for all subjects at all gating windows. As the size of gating window increases from 3 mm to 10 mm, the acceptance probability of the outer k-space segments also increases.

Figure 4A displays the mean and standard deviation of SPR over the 10 under-sampled k-spaces for each subject. Figure 4B shows the SPR in terms of the gating efficiency of each undersampled k-space. Due to the breathing pattern, the gating efficiency differs for different averages and different undersampling pattern is generated. As the gating efficiency reduces, the k-space becomes highly under-sampled and SPR increases. As a point of comparison, ten under-sampled k-space patterns generated by randomly discarding the outer k-space region while keeping the central portion of k-space (for an acceleration rate of 1.75), has average SPR of 0.27 ± 0.01.

Figure 5 shows the reformatted images using retrospective NAV gating and CosMo for gating windows of 3, 5, 7, 10, and 5/10 mm. In this example, the gating efficiencies for CosMo reconstruction for gating windows of 3, 5, 7, 10, and 5/10 mm were 67%, 73%, 78%, 82%, and 76% respectively. CosMo images are highly comparable with the fully sampled acquisition. The mean gating efficiencies range from 47% to 76% for different gating window sizes. Despite an improvement in gating efficiency in the images acquired using a larger gating window of 10 mm for outer k-space, the subjective score did not deteriorate compared to smaller gating window.

Table 1 summarizes the subjective RCA image scores. There is no significant difference between the scores of the images reconstructed by the retrospective gating of the respiratory motion and CosMo.

Table 2 displays the coronary sharpness measure for different gating windows, which demonstrates no significant difference between the retrospective NAV and CosMo.

DISCUSSIONS

In this study, a joint prospective-retrospective NAV, so called CosMo, is implemented and assessed for coronary MRI. The quasi-periodic nature of subject's breathing is used to generate an under-sampled k-space. Subsequently, the motion-corrupted k-space segments were estimated in the reconstruction step using LOST reconstruction. Since CS algorithms require a certain region of inner k-space data to be fully acquired, the proposed prospective-retrospective NAV guarantees acquiring those k-space lines within the gating window by using a prospective diaphragmatic NAV.

While similar scan time can be achieved with an accelerated acquisition using an acceleration factor of 2–3, CosMo results in a fixed and deterministic scan time. There have been several approaches to combine parallel imaging techniques with CS reconstruction to accelerate acquisition (30). In this study, we did not use any parallel acquisition to allow for evaluation of the proposed method and comprehensive study of the under-sampling pattern. However, CosMo can be used with current parallel imaging reconstruction techniques for further reduction in scan time. Further investigation is needed to understand the efficacy of combining CosMo with parallel imaging.

The randomness of the under-sampling pattern generated by CosMo was also studied using a probability map and the SPR of the under-sampling k-space patterns. While the SPR

measure provides a rule-of-thumb for the applicability of compressed sensing, it is inherently tailored for linear reconstruction methods (31) and is signal-independent. Thus, it cannot give a full characterization of the reconstruction process, especially for LOST, which is signal-adaptive. Nonetheless, it provides a simple measure for the incoherency of the under-sampled k-space pattern, and results suggest that the SPR of the pattern generated by CosMo is not very different from that of a randomly generated pattern.

There are significant variations among different patients in terms of breathing pattern and this pattern usually changes during the long scan. In some patients, the under-sampling factor enforced by poor respiratory pattern might be too high for reliable image reconstructions. In these cases, alternative approaches should be used to guarantee a minimal amount of outer k-space data prior to completion of the scan. While this might increase the scan time, it makes sure that the under-sampling will not be too high for image reconstruction. Such approaches need further investigation.

In CosMo, motion-corrupted outer k-space data are completely discarded. However, these data may contain useful information that can improve CosMo reconstruction. Respiratory motion contributes to k-space errors through a variety of effects, e.g. motion relative to the spatially-varying coil sensitivities and non-rigid motion. Nevertheless, the respiratory motion of the heart can be approximated by a time-varying rigid translation. This motion will manifest itself as phase variation in the acquired k-space segment. Therefore, k-space magnitude still carries some useful information and may be utilized to improve reconstruction by adding additional constraint on the magnitude of the estimated k-space lines. This approach needs to be further studied.

We have used diaphragmatic NAV as a surrogate for respiratory motion. However, other methods such as respiratory bellows or fat NAV may also be used.

Our study has several limitations. We have only compared the CosMo reconstructed images with a retrospective NAV gated reconstruction. A prospective NAV gated with tracking is commonly used for coronary MRI. The methodology used in this study to create the reference data, closely simulates a prospective acquisition without any correction (tracking) or adaptive gating. However, gating and tracking will have slightly higher acquisition efficiency compared to gating. Further studies are needed to directly compare the CosMo image acquisition with a prospective NAV gating and tracking. In our current implementation, the size of the fully acquired inner k-space segments was empirically determined. Further studies are needed to systematically study the minimum required number of lines. LOST algorithm with its experimentally chosen parameters was used in CosMo to reconstruct the coronary images and we did not systematically investigate how to optimize LOST's individual parameters. We used objective vessel sharpness and subjective image scores as image quality end-points. These metrics may not reflect the clinical improvements of atherosclerosis lesion detection.

CONCLUSIONS

CosMo acquisition results in randomly unfilled k-space data in coronary MRI that can be estimated in reconstruction step using a CS algorithm, such as LOST, without reacquiring the motion-corrupted data. This approach yields a scan time reduction in coronary MRI.

Acknowledgments

The project described was supported by NIH R01EB008743-01A2, AHA SDG-0730339N and NIH UL1 RR025758-01, Harvard Clinical and Translational Science Center, from the National Center for Research

Resources. Mehdi H. Moghari acknowledges the fellowship support from NSERC (Natural Sciences and Engineering Research Council of Canada).

References

1. Scott AD, Keegan J, Firmin DN. Motion in cardiovascular MR imaging. Radiology. 2009; 250(2): 331–351. [PubMed: 19188310]
2. Wang Y, Vidan E, Bergman GW. Cardiac motion of coronary arteries: variability in the rest period and implications for coronary MR angiography. Radiology. 1999; 213(3):751–758. [PubMed: 10580949]
3. Niendorf T, Hardy CJ, Giaquinto RO, Gross P, Cline HE, Zhu Y, Kenwood G, Cohen S, Grant AK, Joshi S, Rofsky NM, Sodickson DK. Toward single breath-hold whole-heart coverage coronary MRA using highly accelerated parallel imaging with a 32-channel MR system. Magn Reson Med. 2006; 56(1):167–176. [PubMed: 16755538]
4. Edelman RR, Manning WJ, Burstein D, Paulin S. Coronary arteries: breath-hold MR angiography. Radiology. 1991; 181(3):641–643. [PubMed: 1947074]
5. Ehman RL, Felmlee JP. Adaptive technique for high-definition MR imaging of moving structures. Radiology. 1989; 173(1):255–263. [PubMed: 2781017]
6. Taylor AM, Jhooti P, Wiesmann F, Keegan J, Firmin DN, Pennell DJ. MR navigator-echo monitoring of temporal changes in diaphragm position: implications for MR coronary angiography. J Magn Reson Imaging. 1997; 7(4):629–636. [PubMed: 9243380]
7. Wang Y, Rossman PJ, Grimm RC, Riederer SJ, Ehman RL. Navigator-echo-based real-time respiratory gating and triggering for reduction of respiration effects in three-dimensional coronary MR angiography. Radiology. 1996; 198(1):55–60. [PubMed: 8539406]
8. Sachs TS, Meyer CH, Hu BS, Kohli J, Nishimura DG, Macovski A. Real-time motion detection in spiral MRI using navigators. Magn ResonMed. 1994; 32(5):639–645.
9. Oshinski JN, Hofland L, Mukundan S Jr, Dixon WT, Parks WJ, Pettigrew RI. Two-dimensional coronary MR angiography without breath holding. Radiology. 1996; 201(3):737–743. [PubMed: 8939224]
10. Nguyen TD, Spincemaille P, Prince MR, Wang Y. Cardiac fat navigator-gated steady-state free precession 3D magnetic resonance angiography of coronary arteries. Magn Reson Med. 2006; 56(1):210–215. [PubMed: 16767743]
11. Keegan J, Gatehouse PD, Yang GZ, Firmin DN. Non-model-based correction of respiratory motion using beat-to-beat 3D spiral fat-selective imaging. J Magn Reson Imaging. 2007; 26(3):624–629. [PubMed: 17729350]
12. Jhooti P, Keegan J, Firmin DN. A fully automatic and highly efficient navigator gating technique for high-resolution free-breathing acquisitions: Continuously adaptive windowing strategy. Magn Reson Med. 2010; 64(4):1015–1026. [PubMed: 20593372]
13. Lai P, Bi X, Jerecic R, Li D. A respiratory self-gating technique with 3D-translation compensation for free-breathing whole-heart coronary MRA. Magn Reson Med. 2009; 62(3):731–738. [PubMed: 19526514]
14. Pipe JG. Motion correction with PROPELLER MRI: application to head motion and free-breathing cardiac imaging. Magn Reson Med. 1999; 42(5):963–969. [PubMed: 10542356]
15. Stehning C, Bornert P, Nehrke K, Eggers H, Stuber M. Free-breathing whole-heart coronary MRA with 3D radial SSFP and self-navigated image reconstruction. Magn Reson Med. 2005; 54(2):476–480. [PubMed: 16032682]
16. Schmidt, JF.; Buehrer, M.; Boesiger, P.; Kozerke, S. Highly efficient respiratory gating in whole heart MR employing non-rigid retrospective motion correction. Proc 18th Int Soc Magn Reson Med-ISMRM; Stockholm, Sweden. 2010.
17. Hardy CJ, Zhao L, Zong X, Saranathan M, Yucel EK. Coronary MR angiography: respiratory motion correction with BACSPIN. J Magn Reson Imaging. 2003; 17(2):170–176. [PubMed: 12541223]

18. Bhat, H.; Ge, L.; Nielles-Vallespin, S.; Zuehlsdorff, S.; Li, D. 3D projection reconstruction based respiratory motion correction technique for free-breathing coronary MRA. Proc 18th Int Soc Magn Reson Med-ISMRM; Stockholm, Sweden. 2010.
19. Sachs TS, Meyer CH, Pauly JM, Hu BS, Nishimura DG, Macovski A. The real-time interactive 3-D-DVA for robust coronary MRA. IEEE Trans Med Imaging. 2000; 19(2):73–79. [PubMed: 10784279]
20. Manke D, Nehrke K, Bornert P. Novel prospective respiratory motion correction approach for free-breathing coronary MR angiography using a patient-adapted affine motion model. Magn Reson Med. 2003; 50(1):122–131. [PubMed: 12815687]
21. Nehrke K, Bornert P. Prospective correction of affine motion for arbitrary MR sequences on a clinical scanner. Magn Reson Med. 2005; 54(5):1130–1138. [PubMed: 16200564]
22. O'Connor, AC.; Moghari, MH.; Hu, P.; Peters, DC.; Manning, WJ.; Nezafat, R.; Brockett, RW. Retrospective motion-adapted smart averaging for free-breathing cardiac MRI. Proc 18th Int Soc Magn Reson Med-ISMRM; Stockholm, Sweden. 2010.
23. Weiger M, Bornert P, Proksa R, Schaffter T, Haase A. Motion-adapted gating based on k-space weighting for reduction of respiratory motion artifacts. Magn Reson Med. 1997; 38(2):322–333. [PubMed: 9256114]
24. Barral, JK.; Nishimura, DG. Compressed Sensing for Motion Artifact Reduction. Proc 17th Int Soc Magn Reson Med-ISMRM; Honolulu, Hawaii. 2009. p. 4593
25. Lustig M, Donoho DL, Pauly JM. Sparse MRI: The application of compressed sensing for rapid MR imaging. Magn Reson Med. 2007; 58(6):1182–1195. [PubMed: 17969013]
26. Block KT, Uecker M, Frahm J. Undersampled radial MRI with multiple coils. Iterative image reconstruction using a total variation constraint. Magn Reson Med. 2007; 57(6):1086–1098. [PubMed: 17534903]
27. Akcakaya M, Basha T, Goddu B, Goepfert L, Kissinger KV, Tarokh V, Manning WJ, Nezafat R. Low-dimensional-structure self-learning and thresholding (LOST): regularization beyond compressed sensing for MRI reconstruction. Magn Reson Imaging. 2011 (In Press).
28. Kim WY, Danias PG, Stuber M, Flamm SD, Plein S, Nagel E, Langerak SE, Weber OM, Pedersen EM, Schmidt M, Botnar RM, Manning WJ. Coronary magnetic resonance angiography for the detection of coronary stenoses. NEnglJMed. 2001; 345(26):1863–1869.
29. Etienne A, Botnar RM, Van Muiswinkel AM, Boesiger P, Manning WJ, Stuber M. “Soap-Bubble” visualization and quantitative analysis of 3D coronary magnetic resonance angiograms. Magn Reson Med. 2002; 48(4):658–666. [PubMed: 12353283]
30. Lustig M, Pauly JM. SPIRiT: Iterative self-consistent parallel imaging reconstruction from arbitrary k-space. Magn Reson Med. 2010; 64(2):457–471. [PubMed: 20665790]
31. Seeger M, Nickisch H, Pohmann R, Scholkopf B. Optimization of k-space trajectories for compressed sensing by Bayesian experimental design. Magn Reson Med. 2010; 63(1):116–126. [PubMed: 19859957]

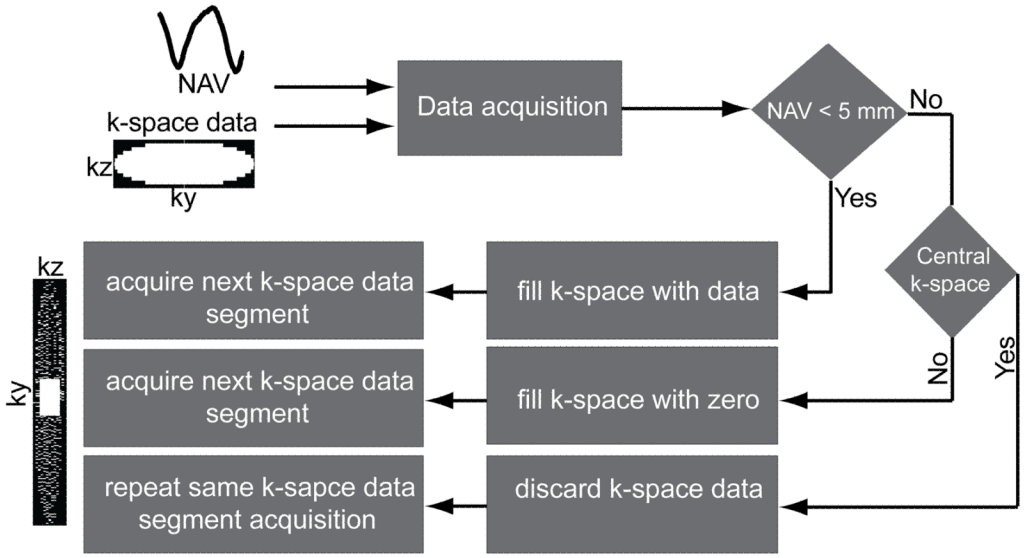

Figure 1.

Schematic of the proposed joint retrospective-prospective NAV scheme for CosMo: inner k-space segments are accepted if the NAV signal is within a pre-specified gating window. Otherwise data are discarded and reacquired in the next cardiac cycle. The outer k-space data are included only if the data are within the acceptance window, otherwise they will be estimated during the reconstruction.

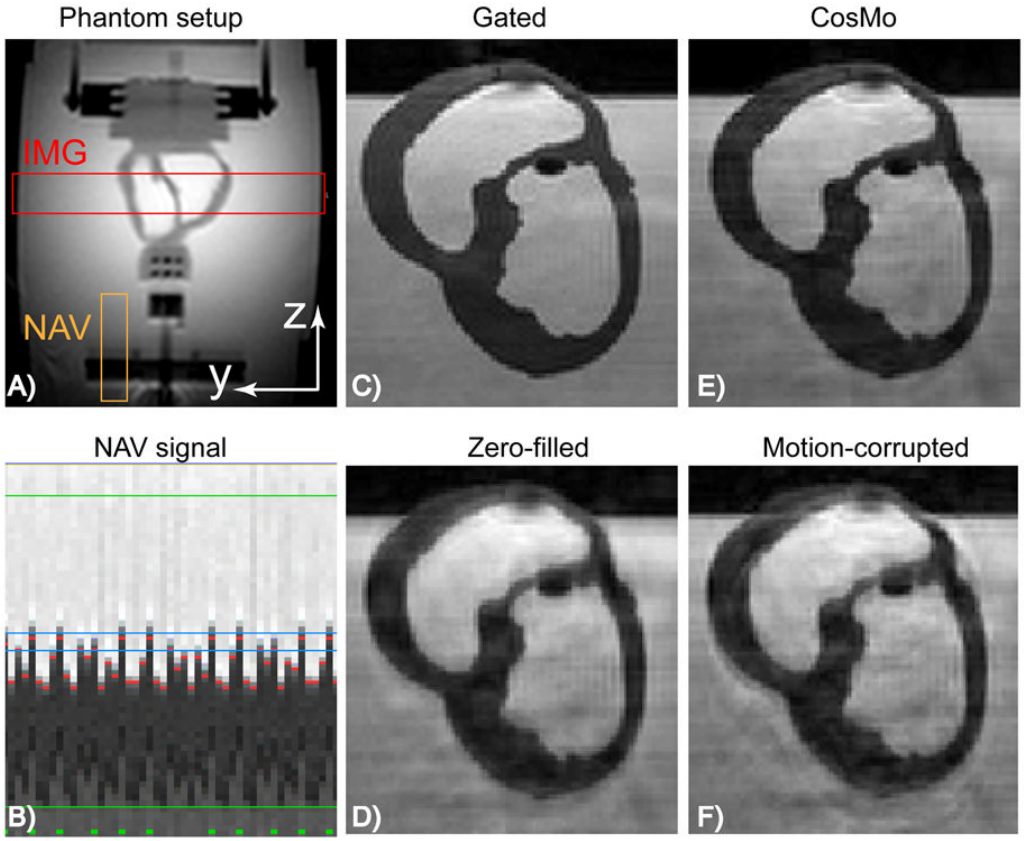

Figure 2.

Non-rigid motion phantom: A) 2D image of the phantom setup demonstrating position of the imaging slab and NAV. B) NAV signal tracking the heart and acquiring the inner k-space lines within 5 mm gating window (after this stage the gating window is increased to acquire the rest of k-space lines). Green, red, and blue lines represent the accepted k-space segments, measured phantom displacements, and gating window size, respectively. C) Prospectively gated NAV with 5mm gating window. D) Zero-filled image, where the outer k-space data acquired outside the gating window are replaced with zero. E) CosMo reconstructed image using 51% k-space data. F) Motion-corrupted image, where the outer k-space data acquired outside the gating window are used in the image reconstruction.

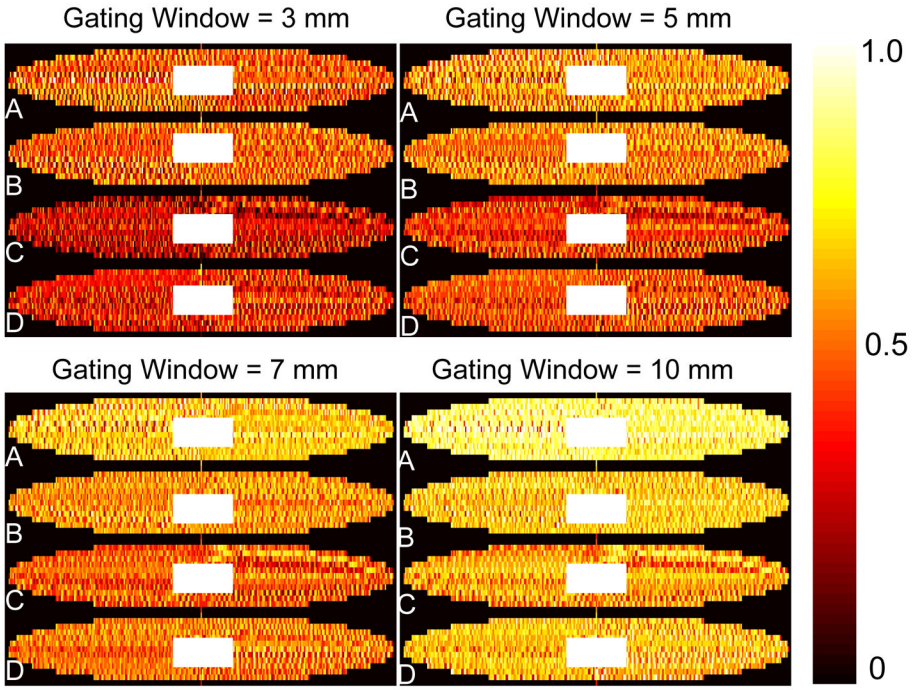

Figure 3.
NAV-generated respiratory under-sampling pattern: the color-map shows the probability of accepted k_y-k_z segments by NAV of four subjects (A–D) for four gating windows (3, 5, 7, 10 mm). The under-sampled lines exhibit randomness between different subjects and for different gating windows.

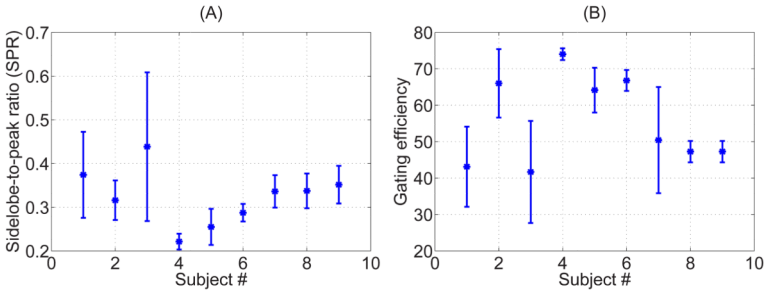

Figure 4.
Mean and standard deviation of the sidelobe-to-peak ratio (SPR) of the under-sampled k-spaces generated within 5 mm gating window for each subject (A), and calculated SPR for calculated gating efficiency (B).

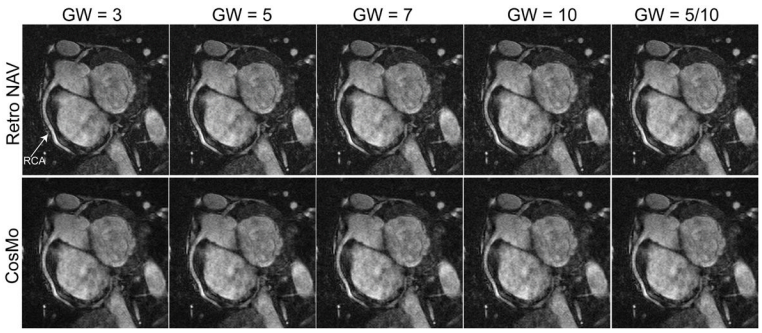

Figure 5.
The reformatted right coronary artery (RCA) images using retrospective NAV and CosMo for different gating windows (GW) of 3, 5, 7, 10 and inner/outer k-space of 5/10 mm. Comparable image quality can be seen between CosMo and NAV gated data.

Table 1

Subjective RCA image scores for retrospective NAV and CosMo with different gating windows for proximal, mid and distal segments. No statistically significant difference was found between the two techniques.

Window Size	NAV Technique	Gating Efficiency	PROX	MID	DIS
3 mm	*Retro NAV*	N/A	3.1±0.6	2.9±0.6	2.4±0.8
	CosMo	47%	3.1± 0.7	2.6±0.9	2.4±0.8
5 mm	*Retro NAV*	N/A	2.8±0.4	2.9±0.6	2.3±0.4
	CosMo	57%	2.8±0.7	2.8±0.8	2.3±0.7
7 mm	*Retro NAV*	N/A	3.1±0.6	2.9±0.6	2.7±0.7
	CosMo	64%	2.6±0.7	2.5±1.0	2.1±0.7
10 mm	*Retro NAV*	N/A	2.6±0.7	2.6±0.7	2.3±0.7
	CosMo	76%	2.5±0.5	2.3±0.8	2.1±0.9
5 mm & 10 mm	*Retro NAV*	N/A	3.0±0.7	3.0±0.5	2.5±0.5
	CosMo	62%	2.8±0.7	2.8±0.8	2.1±0.9

Table 2

RCA sharpness of the images reconstructed with different gating windows using retrospective NAV and CosMo. There was no statistically significant difference between the two techniques with any of gating windows.

Window Size	NAV Technique	Gating Efficiency	Sharpness	Normalized Sharpness
3 mm	*Retro NAV*	N/A	1865±733	0.54±0.07
	CosMo	47%	1537± 632	0.5±0.08
5 mm	*Retro NAV*	N/A	1661±523	0.52±0.08
	CosMo	57%	1424±560	0.49±0.09
7 mm	*Retro NAV*	N/A	1834±695	0.53±0.07
	CosMo	64%	1424±560	0.49±0.08
10 mm	*Retro NAV*	N/A	1778±761	0.51±0.08
	CosMo	76%	1512±650	0.48±0.09
5 mm & 10 mm	*Retro NAV*	N/A	1836±707	0.52±0.08
	CosMo	62%	1548±568	0.49±0.08